Available online a**t** www.pelagiaresearchlibrary.com

Pelagia Research Library

Advances in Applied Science Research, 2014, 5(5):12-18

ISSN: 0976-8610
CODEN (USA): AASRFC

Gas sensing properties of nanocrystalline silver/tin dioxide sensor prepared by coprecipitation method

Shivanand G. Sonkamble[a*] and Anil B. Gambhire[b]

[a]*Pratishthan Mahavidyalaya, Paithan, Aurangabad (MS), India*
[b]*Department of Chemistry, Shri Anand College of Science, Pathardi, Ahmednagar (MS), India*

ABSTRACT

Nanosize tin dioxide based powders containing silver oxide and palladium have been prepared by coprecipitation reaction. The material obtained is nanocrystalline, having particle size in the range from 5.21 to 7.42 nm and decreases with increasing amount of doping silver. High selective and sensitive thick-film gas sensors were fabricated and their sensing characteristics for H_2S and other toxic gases were investigated at the operating temperature of 70°C. Pd-added, silver doped-SnO_2 thick-film sensor exhibited high sensitivity to H_2S gas of 1-10 ppm and had good selectivity to H_2S gas than that of the other gases (1000 ppm). This material (Pd + Ag_2O/SnO_2, Pd = 1.5 wt. %, Ag = 3 wt.% sintered at 600°C with an optimal temperature of 70°C) may prove to have tremendous potential for H_2S gas sensing applications.

Keywords: Nanomaterials; Thick-film; Tin dioxide; Silver; H_2S; XPS

INTRODUCTION

Hydrogen sulfide is a colorless, toxic, flammable gas that is responsible for the foul odor of rotten eggs and flatulence. It often results when bacteria break down organic matter in the absence of oxygen, such as in swamps, and sewers. H_2S-producing bacteria also operate in the human colon, and the odor of flatulence is largely due to trace amounts of the gas. About 10% of total global emissions of H_2S are due to human activity. By far the largest industrial route to H_2S occurs in petroleum refineries. Other anthropogenic sources of H_2S include cock ovens, paper mills (using the sulphate method), and tanneries. The threshold level is believed to average around 300-350 ppm. Personal safety gas detectors are set to alarm at 10 ppm and to go into high alarm at 15 ppm. Therefore, much attention has been paid to the search for H_2S gas sensitive material [1-4].

Semiconductor metal oxide chemical sensors have been widely used for detecting combustible or toxic gases particularly for low cast and a lower operating temperature [5]. It is belived that sensor sensitivity can be improved by increasing the sensor surface areas so that it will provide more surface sites available for gas to adsorbed on these sites and to make contact with the surrounding gases. Therefore, it is essential to improve the sensitivity and selectivity by means of the use of doping, the use of promoters, specific surface additives, filters and operating temperature [6-9].

The utilization of heterogeneous interface between CuO/SnO_2 [10], CeO_2/SnO_2 [4], for the selective detection of H_2S gas less than 5 ppm is documented in the literature. Especially, sensor materials based on SnO_2 with Ag as a catalyst have been extensively studied using thin film structure [11, 12], chemically fixed Ag_2O on SnO_2 film [13], and SnO_2-Ag-SnO_2 composite film gate MIS diodes [14]. However, for the above H_2S gas sensors [4, 10-13] high working temperatures are needed for them. They have a long response, recovery time [11], and existing cross sensitivity [14]. Ag/SnO_2 nanocomposite, with quick response and recovery behavior upon exposure to H_2S as low as 1 ppm at working temperature as low as 70°C, prepared by the sol-gel method, has been reported [15]. The high performance has been shown to beginning from electronic and chemical characteristics of silver, which has a larger electronegativity difference to sulfur than tin atom and has a strong tendency to form a p-n junction. The aim and objective of the present investigation is to study the effect of addition of Ag (Ag = 1, 2, and 3 wt. %) and Pd (fixed at 1.5 wt.%) promoters on the gas sensing performance of SnO_2 under the identical conditions wherein very high values for both the sensitivity and selectivity were obtained. The powder composition was selected keeping in view the role of Pd as a catalyst and the role of Ag (an "p" type dopant which goes into solid solution with SnO_2) in lowering the sensors resistance within acceptable limit for real life applications. The sensitivity and selectivity to H_2S of the sensing thick-films were investigated at the operating temperature of 70°C and the results were compared with those to other gases (CO, CO_2, LPG, and H_2).

MATERIALS AND METHODS

2. 1. Powder and thick-film preparation

The reagent grade chemicals used in preparing the samples, stannic (IV) chloride ($SnCl_4$, 99.9% Qualigen), silver acetate ($AgOOCCH_3$, Merk) and palladium (II) chloride ($PdCl_2$, Merk), as a starting materials. Silver (I) acetate solution ($AgOOCCH_3$) was dissolved in C_2H_5OH and PEG as a surfactant was added into $SnCl_4$ to obtain a $SnCl_4$ solution. The $AgOOCCH_3$ solution in the ethanol with NH_4OH was dropped into the $SnCl_4$ solution to form the precipitate, respectively. Then the precipitate was thoroughly washed with dilute NH_4NO_3 solution and dried at 100°C to form the precursors. In this process the pH value of 7 was sustained. From the result of TG-DTA analysis, the calcination temperature was fixed at 500°C.

The thick-film gas sensor device consisting of a combined Pd to the raw material, Ag_2O/SnO_2 has been developed for detection of H_2S gas. Mixture of Ag and Pd has been found to be more efficient catalyst to alleviate the phase transition as compared to using Ag only [16]. The electrode prepared by screen-printing method comprising combining a base component (alumina substrate) with a metal paste (RuO_2 and Pt paste) and heating the paste in the presences of air for a time sufficient to oxidize a portion of the electrode to produce the metal/metal oxide electrode. Sensing electrodes were formed with metal paste on the opposite side. Hence, the sensing material was formed between the electrodes were sintered at 600°C, 1 h in air. The fabrication method of the H_2S gas sensor device was similar to the previously reported one [9].

2. 2. Characterization

X-ray powder diffraction (XRD) patterns were taken at room temperature (RT) using a model D8 Bruker AXS using monochromatic Cu radiation (40 Kv and 30mA).

The Fourier transform infrared spectroscopy (FT-IR) analysis was performed using a Shimadzu-8400 spectrometer. Thermogravimetry and differential thermal analyses (TG-DTA) were performed by Mettler-Toledo, TGA-SDTA 851.Transmition electron microscopy (TEM) measurements were carried out on a JEOL Model 1200EX instrument operated at an accelerating voltage of 100 kV. X-ray photoelectron spectroscopy (XPS, ESCA-3000-VG Microtech England) was used to study the chemical composition of the sample. The sensing performance of the sensors was examined using "injective-type" sensing system. The H_2S response tests were carried out with a PC-controlled measuring system. Sensors to be tested were placed in a measuring chamber of about 0.5 dm^3 in volume. Optimum detection temperature were determined and the thick-film sensors maintained at this fixed temperature were exposed to varying test gas (in the range 1-10 ppm), using a gas flow controller unit with an air flow rate of 0.5 dm^3/min. Response, S, to gas is defined as $S = R\ (air)/R\ (gas)$, where $R\ (air)$ is the sensor resistance in clean air and $R\ (gas)$ is the resistance in the test gas.

RESULTS AND DISCUSSION

3.1 Structural properties

In order to understand the phase symmetry in the thick-film sintered at 600°C temperature, a systematic study on the X-ray diffraction was undertaken. Fig.1 show XRD pattern for pure SnO_2 thick-film, sintered at 600°C for 1 h in air reveals the tetragonal phase, which is dominant and together with the orthorhombic phase giving the rise to only three very weak peaks. Kersen et al. [17] have concluded that dehydration of the surface of SnO_2 occurs principally via condensation of adjacent surface hydroxide groups on the (100) plane with secondary condensation on the (101) plane. Hydroxide group condensation on these planes will lead to the formation of surface Sn-O-Sn bridges. It was concluded that a possible factor, affecting the sensitivity to gases, is the formation of strong Sn-O-Sn stretching mode deformation.

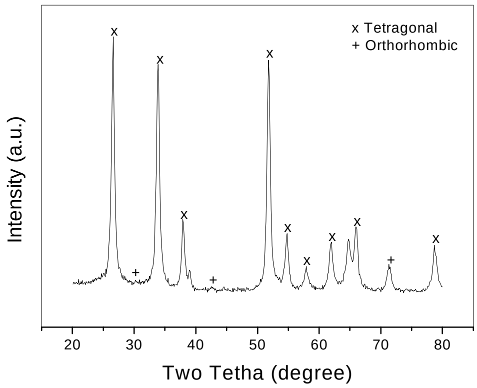

Fig. 1. X-ray diffraction pattern of the synthesized SnO_2 thick-film with typical distribution of the tetragonal and orthorhombic phases

Fig. 2(a-c) shows the XRD patterns of thick-films (a) 1 wt.% Ag_2O/SnO_2, (b) 2 wt.% Ag_2O/SnO_2, and (c) 3 wt.% Ag_2O/SnO_2 with the fixed Pd amount of 1.5 wt.%, sintered at 600°C for 1 h in air. In all cases, the peak positions agree well with the reflections of bulk polycrystalline SnO_2 with tetragonal symmetry [18]. No other phases have been detected, indicating that all Ag and Pd come into the crystal lattice of bulk SnO_2 to substitute for Sn ions. All diffraction lines are broadened, indicating nanosized crystallites in the samples. The width increases with the increase of silver-doping level. It can be expected that the particles are completely depleted in electrons and very high gas sensitivity will be achieved. The particle size after sintering did not show much change. Therefore, to analyze the relationship between the particle size and sensitivity, we examined the particle size effect. The average particle sizes of the powder were calculated using Debye-Scherrer formula [19].

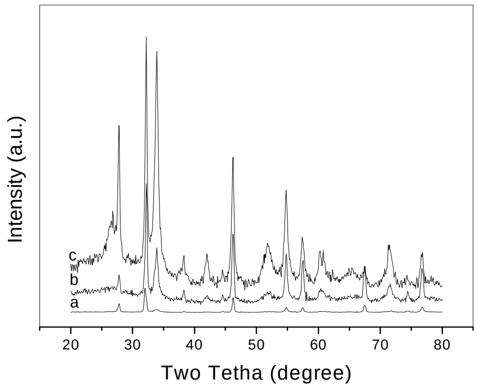

Fig. 2. X-ray diffraction patterns of thick-films (a) 1 wt.% Ag_2O/SnO_2 (b) 2 wt.% Ag_2O/SnO_2, and (c) 3 wt. % Ag_2O/SnO_2 with the fixed Pd amount of 1.5 wt.%, sintered at 600°C for 1 h in air

It was shown that the average particle sizes of the nanocrystalline powders decreases with increasing amount of doping Ag_2O. The average particle size is form 5.21 to 7.42 nm. This apparent fall in average particle size (higher surface area) indicates the possible reason for the maximum sensitivity for the samples with 3 wt.% of Ag_2O.

Table 1 The variations of particle size of SnO_2

*Doping amount (wt. %)	0	1	2	3
D [nm]	7.92	7.42	6.02	5.21
d (110) [nm]	0.3345	0.3635	0.3550	0.3226

**Sintered material, Pd (1.5 wt. %) + Ag_2O/SnO_2.*

From the XRD patterns, the effect of the silver-doping quantities with the fixed Pd amount on the average particle size and the (110) *d*-spacing is shown in Table 1.

3.2 FT-IR spectra

Fig. 3(a-d) shows the FT-IR spectra of thick-films (a) pure SnO_2, (b) 1 wt.% Ag_2O/SnO_2, (c) 2 wt.% Ag_2O/SnO_2, and (d) 3 wt.% Ag_2O/SnO_2 with the fixed Pd amount of 1.5 wt.%, sintered at 600°C for 1 h in air. The spectra show that SnO_2 spectrum (Fig. 4a) is similar to the other sample (Fig. 4b-d) which is doped with silver.

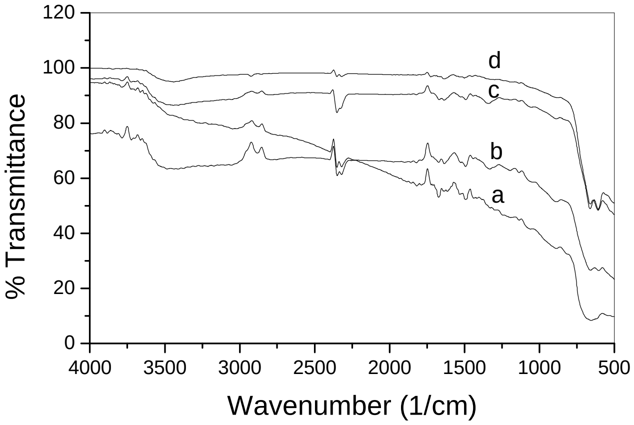

Fig. 3. FT-IR spectra of thick-film (a) pure SnO_2 (b) 1 wt.% Ag_2O/SnO_2 (c) 2 wt.% Ag_2O/SnO_2 (d) 3 wt. % Ag_2O/SnO_2 with the fixed Pd amount of 1.5 wt. %, sintered at 600°C for 1 h in air

A broad absorption band in the range 3750-2500 cm^{-1} is due to the asymmetric hydroxide stretching mode and the band between 820 and 1300 cm^{-1} is assigned to the hydroxide deformation mode. The molecular water deformation mode is located at 1640 cm^{-1}. The band at 1450 cm^{-1} is most probably an overtone of the asymmetric Sn-O-Sn stretching mode of a surface-bridging oxide formed by condensation of adjacent surface hydroxide groups. The SnO_2 stretching vibrations are observed at 625 cm^{-1} and lattice modes of SnO_2 appears at 690 cm^{-1}. Fig. 4(a and b-d) are matching with each other. This reveals that Ag and Pd dissolved into the SnO_2 lattices and form a solid solution. These results are in agreement with the XRD points.

3.3 Microstructural analysis

Fig. 4(a-b) shows the TEM micrograph of 3 wt. % Ag_2O/SnO_2 nanocrystalline powder sintered at 600°C for 1 h in air and the electron diffraction pattern, which confirms the nanometric size of the particles. It is shown that the morphology of nanocrystalline silver-doped SnO_2 particle is basically spherical, and the crystal size distribution of sample is uniform. The crystal size measured by TEM is accordance with that of the sample examined by XRD. Compared with the chemically pure SnO_2, CuO/SnO_2 and CeO_2/SnO_2, the Ag_2O/SnO_2 nanoparticles in the present work has nanosize microstructure and uniform size distribution, it is greatly good for the selectivity and sensitivity of the chemical sensors.

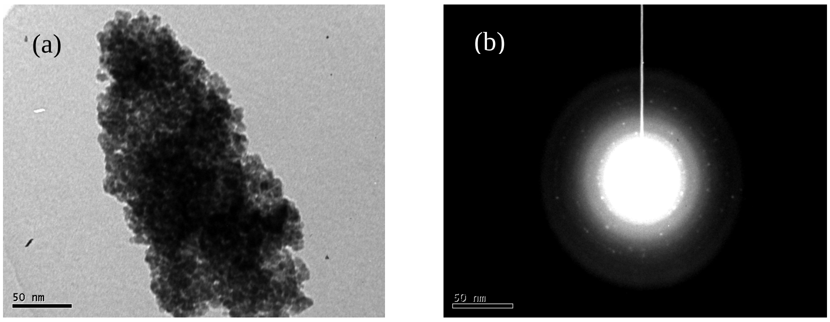

Fig. 4(a-b) TEM micrograph of the sample 3 wt. % Ag_2O/SnO_2 containing Pd fine particles prepared by the coprecipitation method, sintered at 600°C for 2 h in air

As shown in Fig. 5(a-c), Ag3d, Sn3d and Pd3d high resolution XPS spectra of as-prepared thick-films show peak position at binding energies of 368.0 and 487.4 eV that correspond to pure Ag_2O and SnO_2 [20, 21], respectively. The spectra of Pd3d level is very broad and shows the asymmetric towards higher binding energy side. The spectra could be deconvoluted into two components with respective binding energies of 335.0 and 336.1 eV. The binding energy value of first and second peak is well matching with the reported binding energy value of Pd [22], corresponding to Pd of different oxidation states; Pd^0 and Pd^{+2}. The reduction of Pd^{+2} to Pd^0 might be due to metal-metal oxide interaction at higher temperature. However, at least a part of Pd is not incorporated into polycrystalline SnO_2 and remains as separate phase, which is reduced to Pd^0 at 500°C. XPS study reveled the presence of Pd^{+2}, which indicate a reoxidation of Pd^0 in the surface layer during cooling. Fig. 5(d) exhibited the XPS spectra for the O1s region. The O1s peak shows broadening here too the spectra could be deconvoluted into two components. The binding energies values are 530.5 and 533.8 eV respectively. These are assigned as O^{2-} from oxides and OH^{-} species preset on the surface respectively. It is concluded that the ratio of O^{2-}/OH^{-} and higher dispersion of Pd^{+2}/Pd^0

sites may represents the relative gas adsorption capability of Ag_2O/SnO_2 thick-film sintered at 600°C and can be derived to obtain a relative concentration of surface adsorption sites, which adsorbed oxygen will initially occupy.

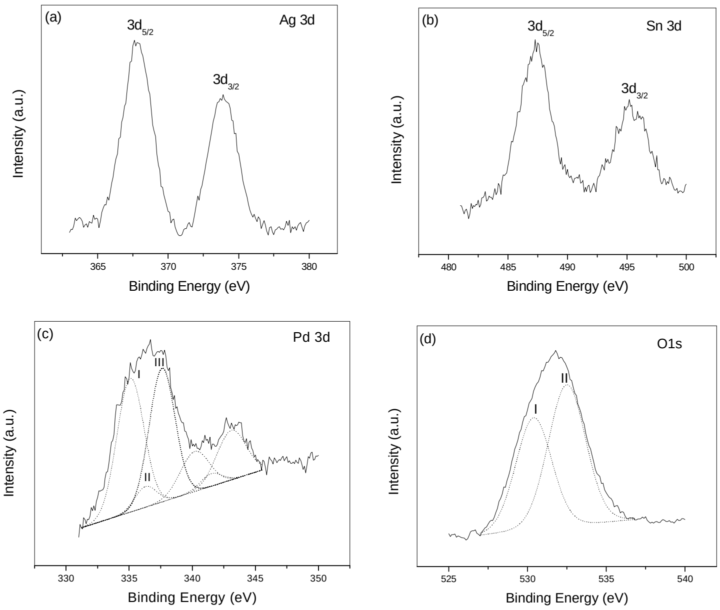

Fig. 5. High resolution XPS spectra of 3 wt.% Ag_2O/SnO_2 thick-film with the fixed Pd amount of 1.5 wt.% (a) Ag3d XPS spectra, (b) Sn3d XPS spectra, (c) Pd3d (d) O1s XPS spectra, sintered at 600°C for 1 h in air

3.4 Sensing characteristics of the Ag_2O/SnO_2 composite thick-films

Fig. 6 shows the gas sensitivities with Ag concentration (1, 2, and 3 wt.%), thick-film sintered at 600°C to H_2S gas at concentration of 1 ppm. The gas sensitivity of three kinds of silver-doped SnO_2 film showed high sensitivity to H_2S gas at the operating temperature of 70°C. The maximum values have relation to the particle size in the thick-film. For the thick-films with D = 6.02 and 5.21 nm, very high sensitivity was achieved, as shown in Fig. 6(c) and 6(d). The particle size for the sample with 3 wt.% Ag_2O/SnO_2 is smaller than the rest of the samples.

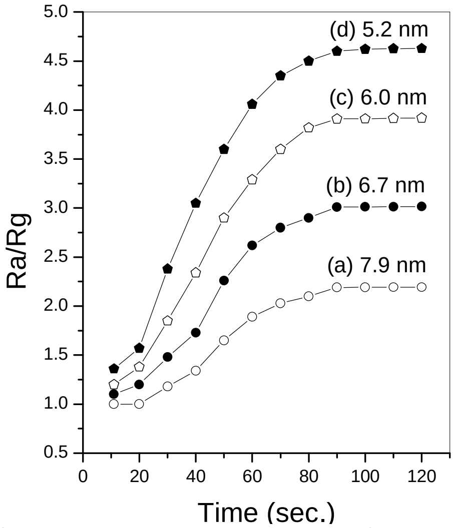

Fig. 6. Response transients of sensing thick-films to 1 ppm H_2S at 70°C with wt. % of Ag. (a) pure SnO_2 (b) 1 wt.% Ag_2O/SnO_2 (c) 2 wt.% Ag_2O/SnO_2 (d) 3 wt.% Ag_2O/SnO_2, with the fixed Pd amount of 1.5 wt.%

The high sensitivity is due to the dispersion of Ag and Pd promoters, the oxides (Ag_2O and PdO) formed in air interact with the SnO_2 surface to produce an electron-deficient space-charge layer. The sensor with 3 wt.% Ag_2O/SnO_2 was observed to be most sensitive and shows a high resistivity in air, which drastically drop in the presence of hydrogen sulfide. This could be attributed to optimum number of p-n heterojunctions formed on the surface, which induces an electron-deficient space-charge layer at the surface of the thick-film. It is evident from the XPS study, a lot of adsorbed O^{2-}/OH^{-} on a SnO_2 surface. The presence of chemisorbed oxygen also may cause electron-deficient space-charge layer in the thick-film surface and the building up of a Schottky surface barrier; as a result, the electrical resistance of the thick-film decreased to a minimum value. Moreover, the sharp increase of gas sensing over the 3 wt.% Ag_2O/SnO_2 sample with lower content of Pd at about 70°C was ascribed to the higher dispersion of Pd^{+2} and Pd^0 phases. Thus, the higher contribution of lattice oxygen and possible local change in oxidation state of Pd can be a reason for the enhanced sensitivity. To what extent, the above effects dominate the general theory for optimization of concentration (wt. %) of additives needs further experimentation. However, in our work, we have added Ag metal in SnO_2 which on sintering gives Ag_2O/SnO_2 system with tetragonal phase of SnO_2 at optimized concentration of 3 wt.% of Ag with the fixed Pd amount of 1.5 wt.%. Further, the best selectivity values for H_2S were observed at 2 wt. % of Ag.

Fig. 7 shows the sensitivities of the 3 wt. % Ag_2O/SnO_2 thick-film sintered at 600°C to H_2S gas at concentrations of 0.1, 0.5, 1, 5, and 10 ppm. The fabricated Ag_2O/SnO_2 thick-film showed high sensitivity to H_2S gas in the concentration of 1-10 ppm at the operating temperature of 70°C.

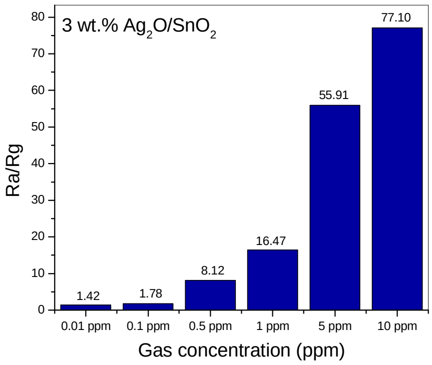

Fig. 7. Sensitivity of the 3 wt. % Ag_2O/SnO_2 thick-film sintered at 600°C as a function of H_2S gas concentration

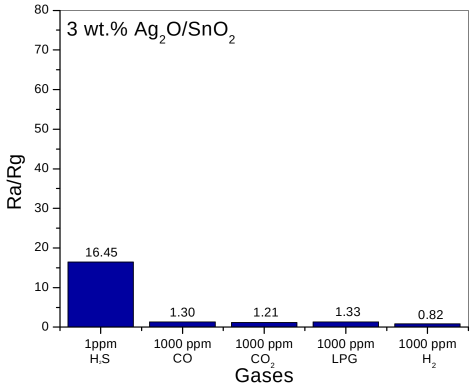

Fig. 8. Selectivity of 1 ppm H_2S gas

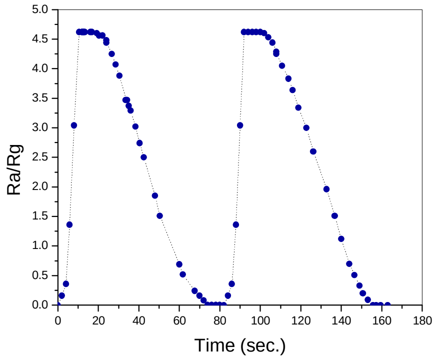

Fig. 9. Response and recovery of 3 wt. % Ag_2O/SnO_2 thick-film upon exposure to 1 ppm H_2S at 70°C

Fig. 8 shows the variation of selectivity with 3 wt. % Ag_2O/SnO_2 thick-film for H_2S (1 ppm) to other gases such as CO, CO_2, LPG and H_2 of 1000 ppm. The high selectivity to H_2S gas at 70°C seems to be due to Ag_2O reacts to produce the corresponding Ag_2S, the tarnish that forms on silver when exposed to the hydrogen sulphide gas. This produce no major change in response due to interfering gases used additionally. The 3 wt. % Ag_2O/SnO_2 thick-film revealed high response and recovery times. As it can be seen in Fig. 9, the thick-film have quick response (10 s) towards 1 ppm of H_2S gas at 70°C, and the sensor could recover within 60 s after heating at 120°C.

CONCLUSION

Our studies on Ag_2O/SnO_2 gas sensor system revealed that

1. The silver-doped SnO_2 nanoparticles were prepared by the coprecipitation reaction and subsequent thermal treatment from the silver acetate and tin chloride.
2. The average particle is in the range from 5.21 to 7.42 nm. It is shown that the average particle size of the nanoparticles decreases with amount of silver-doping.
3. The thick-film gas sensor prepared with Ag_2O/SnO_2 material exhibited good sensitivity, high selectivity, and quick response and recovery behavior toward low concentration of H_2S at 70°C.
4. These high sensitivity and wider rang characteristics are achieved by using Ag and Pd additive with a higher surface area due to small average particle size which is expected to increase the formation of p-n heterojunctions and adsorption of O^{2-}/OH^{-} species on a SnO_2 surface to produce an electron-deficient space-charge layers.
5. The thick-film sensor with 3 wt.% Ag could detect H_2S gas concentration as low as 0.01 ppm, which is less than its occupational exposure limit.
6. The surface properties of silver-doped SnO_2 nanocrystalline powder have been examined using XPS with regard to H_2S gas sensor. A higher Ag, Pd and SnO_2 fractions are found to be present on the surface of sensing materials suggests that the enrichment in Ag, Pd and SnO_2 sites in the sensing characteristics of the sensor.

Acknowledgement

We are very much thankful to Late Dr .V.G.Dongre Professor, Department of Chemistry, Mumbai University, Mumbai and Late Dr .V.W.Kamble, Deputy Director, Forensic Lab, and Aurangabad for his valuable guidance and supports for research work.

REFERENCES

[1] Kanefusa S, Nitta M, Haradome M, *IEEE Trans. Electron Devices* ,**1998**, 35 , 65.
[2] Solis J, Saukko S, Kish L, Grangvist C, Lantto V. *Sens Actuators* B **2001**, 77, 316.
[3] Jain G, Patil L,Wagh M, Patil D, Patil S, Amalnerkar D. *Sens Actuators* B **2006**,117, 159.
[4] Fang G, Liu Z, Liu C, Yao K. *Sens Actuators* B **2000**,66, 46.
[5] Haugen J, Kvaal K, Meat. *Sci.* **1998**, 49, 273.
[6] Wu Z, Shen G, Xie L, Yu R, PEG *Sens. Actuators*. **2012**,B 71 , 99.
[7] Semancik S, Fryberger T, *Sens. Actuators.* **1990**, B, 1 97.
[8] Kwon C, Yun D,Hong H,Kim S,Lee K, Lim H,Yoon K, *Sens. Actuators.* **2011**, B 65 327.
[9] Sung J, Lee Y Lim J, Hong Y, Lee D, *Sens. Actuators*. **2000**,B 66, 149.
[10] Lee J, Moon B, Shim C, Kim B, Lee M, Lee D, Lee J, *Sens. Actuators* **2005**,B 108, 84.
[11] Mizei J, *Sens. Actuators* **1993**,B 15-16 , 328.
[12] Liu C, ZhangL, He, Y, *Thin Solid Films* **1997**, 30413.
[13] JianpingL, Yue W, Xiaoguang G,Qing M, Jinghong H, , *Sens. Actuators* **2000**' B 65 '111.
[14] http://www.people.cecs.ucf.edu/sseal/nano.htm#silver.
[15] Gong J, Chen Q, Lian M, Li N, Stevenson R, Adami F, *Sens. Actuators* **2010**, B 114, 32.
[16] Zalvidea D, Diez A, Cruz J, Andres M, *Sens. Actuators*. **2006**, B 114, 268.
[17] Kersen U, Sundberg M, *J. of the Electrochem. Soc.*, **2003**,150 6 H129-H134.
[18] Cullity B, , *Addison-Wesley*, London, **1978**.
[19] Taylor A, *John Wiley, New York*, **1961**,pp. 678, 686.
[20] Moller D, Pham M, Huller J, *Sens. Actuators*. **1997**, B 43, 110.
[21] Lavacchi A, Cortigiani B, Rovida G, Bardi U, Atrei A, Angelucci R, Dori L, Nicoletti,S, *Sens. Actuators*. **2013**, B 71 123.
[22] Petrovic S, Karanovic L, Stefanov P, Zdujic M, Baricevic A, *Appl. Catalysis*. **2005**,B 58 , 133.